Dalton Transactions

PAPER

View Article Online
View Journal | View Issue

Cite this: *Dalton Trans.*, 2016, **45**, 3874

A niobium-necked cluster $[As_3Nb(As_3Sn_3)]^{3-}$ with aromatic Sn_3^{2-} †

Fu-Xing Pan,‡[a,b] Cong-Qiao Xu,‡[c] Lei-Jiao Li,[a] Xue Min,[a,b] Jian-Qiang Wang,[d] Jun Li,*[c,e] Hua-Jin Zhai[f] and Zhong-Ming Sun*[a]

Received 4th January 2016,
Accepted 19th January 2016

DOI: 10.1039/c6dt00028b

www.rsc.org/dalton

We describe here the synthesis and characterization of a ternary cluster compound $[As_3Nb(As_3Sn_3)]^{3-}$ (**1**), in which a niobium(v) atom is coordinated by an As_3^{3-} triangle and a bowl-type $As_3Sn_3^{5-}$ ligand. Cluster **1** was synthesized by dissolving $K_8NbSnAs_5$ (**2**) in the presence of [2.2.2]crypt in ethylenediamine solution, filtered and layered with toluene, then crystallized in the form of $[K([2.2.2]crypt)]_3[As_3Nb(As_3Sn_3)]\cdot en\cdot tol$. The flower-vase shaped compound **1** features a new structure type, rather different from the known Zintl phases. The stability and bonding of **1** are elucidated *via* extensive bonding analyses. The Sn_3 ring is found to have σ-aromaticity featuring a delocalized Sn–Sn–Sn σ bond. Electronic structure calculations confirm the Nb(v) oxidation state and weak Nb–Sn and Sn–Sn bonding, in addition to the normal Nb–As and As–As bonds.

1. Introduction

The bridge between solution and solid chemistry of Zintl clusters has been established for more than 80 years.[1] A variety of homo and binary p-block polyanions such as E_9^{4-} (E = Ge, Sn) and $Sn_2Bi_2^{2-}$ have been extracted from salt-like precursors.[2] The report of *closo*-$Sn_9Cr(CO)_3^{4-}$ by Eichhorn and co-workers triggered a new direction by introducing d-block metals into the polyanions,[3] leading to the formation of clusters with unique geometries and electronic structures.[4] Notably these include the onion-skin like $[As@Ni_{12}@As_{20}]^{3-}$, $[M@Pb_{12}]^{2-}$ (M = Ni, Pt, Pd), and endohedral "stannaspherene" $[Ir@Sn_{12}]^{3-}$.[5–9]

Group 15 polyanions Pn_7^{3-} (Pn = P, As) have also been successfully activated by a Co(II) complex "where the nuclearity of the heptaphosphide starting material remains the same but where a significant alteration of the nortricyclane-like cage geometry has resulted".[10] As for their heavier congeners, some anions with lower nuclearities such as Sb_n^{n-} (n = 3, 5) and Bi_n^{n-} (n = 2, 3) can be isolated or stabilized by transition metals (TMs), proving the existence of Pn_n^{n-} (Pn = Sb, Bi) in solutions.[11a–c] Notably, Bi_n^{3-} (n = 7, 11) were obtained recently in the presence of Cr and Ga, respectively.[11d,e] On the other hand, TMs may also serve as oxidation agents, for example, Pb_{10}^{2-} was obtained through Pb_9^{4-} as oxidized by a Au(I) precursor.[12] Apart from d-block embedding Zintl clusters, f-block elements have also been introduced into the Sn–Bi, Pb–Bi, In–Bi and Ga–Bi systems.[13]

The above clusters, also named as "intermetalloid clusters", a concept introduced by Fässler,[14] greatly enrich the family of Zintl phases and provide understanding of metal–metal bonding interactions. However, compared with the diverse electron-rich TM and rare-earth metal embedded anions, isolated clusters with electron-deficient TM atoms are mainly metal carbonyl complexes, except for $[MPn_8]^{n-}$ (M = Cr, Mo, Nb; Pn = As, Sb; n = 2, 3) and $[(\eta\text{-}C_6H_5Me)NbSn_6Nb(\eta\text{-}C_6H_5Me)]^{2-}$.[4b,15] Recently, a series of Ti–Sn clusters with a cyclopentadienyl ligand were synthesized in liquid ammonia.[16] "Extremely hard cations" of M^{5+} (M = V, Nb) were encapsulated in the Ge–As cages to form $[V@Ge_8As_4]^{3-}$ and $[Nb@Ge_8As_6]^{3-}$, respectively.[17] Besides Zintl clusters, electron-deficient TMs were also used in the activation of P_4.[18] In general, ligand-free Zintl clusters embedding electron-deficient TM atoms are still poorly explored. In this paper, we report a

[a]*State Key Laboratory of Rare Earth Resource Utilization, Changchun Institute of Applied Chemistry, Chinese Academy of Sciences, Changchun, Jilin 130022, China. E-mail: szm@ciac.ac.cn*
[b]*University of Chinese Academy of Sciences, Beijing 100049, China*
[c]*Department of Chemistry & Key Laboratory of Organic Optoelectronics and Molecular Engineering of Ministry of Education, Tsinghua University, Beijing 100084, China. E-mail: junli@tsinghua.edu.cn*
[d]*Shanghai Institute of Applied Physics, Chinese Academy of Sciences, Shanghai 201800, China*
[e]*William R. Wiley Environmental Molecular Sciences Laboratory, Pacific Northwest National Laboratory, Richland, Washington 99352, USA*
[f]*Nanocluster Laboratory, Institute of Molecular Science, Shanxi University, Taiyuan 030006, China*

†Electronic supplementary information (ESI) available: Experimental procedures, EDX and powder X-ray diffraction analyses results, mass spectra and structural parameters of both compounds. Optimized geometric parameters, charges, bond orders, NICS values, and bonding analysis results. CCDC 1012141. For ESI and crystallographic data in CIF or other electronic format see DOI: 10.1039/c6dt00028b

‡These authors contributed equally to this work.

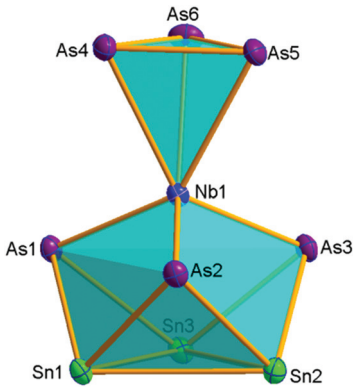

Fig. 1 Thermal ellipsoid plot of $[As_3Nb(As_3Sn_3)]^{3-}$ (drawn at 50% probability). Selected bond distances (in Å): Nb1–As1–3, 2.558(1)–2.584(1); Nb1–As4–6, 2.770(1)–2.791(1); Sn–Sn, 3.123(1)–3.145(1); Sn–As, 2.735(1)–2.775(1); As–As, 2.416(1)–2.437(1). Bond angles within the As_3 and Sn_3 triangles (in degrees): 59.66(3)–60.51(3); 59.65(2)–60.33(2).

niobium-necked ternary Zintl cluster $[As_3Nb(As_3Sn_3)]^{3-}$ with an entirely new structure type (Fig. 1), which was characterized in $[K([2.2.2]crypt)]_3[As_3Nb(As_3Sn_3)]\cdot en\cdot tol$.

2. Results and discussion

As shown in Fig. 1, the $[As_3Nb(As_3Sn_3)]^{3-}$ cluster consists of an As_3 triangle, a Nb atom, and a bowl-type As_3Sn_3 unit. The Nb atom is situated in the central position, bridging the top As_3 triangle and the bottom As_3Sn_3 unit. The top As_3 ligand is reminiscent of those in $[P_3Nb(ODipp)_3]^-$, $[Co(\eta^3\text{-}As_3)\{\eta^4\text{-}As_4(mes)_2\}]^{2-}$, $[Co_6As_{12}(PEt_2Ph)_6]$, $[Pd@Pd_2Pb_{10}Bi_6]^{4-}$, and $[Sb_3Au_3Sb_3]^{3-}$,[10b,19] and it is almost parallel to the bottom Sn_3, with a small dihedral angle of 2.4°. All bond angles within the two triangles are 60 ± 0.51°. The torsion angles between $AsSn_2$ and Sn_3 faces are around 130°. The Sn–Sn distances within the Sn_3 triangle are in the range of 3.123–3.145 Å, which are relatively long for a normal Sn–Sn single bond (2.80 Å in α-Sn), but comparable to those in $[Pd_2@Sn_{18}]^{4-}$ (3.012–3.145 Å).[20] The Nb–Sn distance is around 3.29 Å, which is slightly beyond the normal distance of effective bonding interaction. The Sn–As bonds in As_3Sn_3 range from 2.735 to 2.775 Å, which are comparable to those in $[SnAs_{15}]^{3-}$ (2.647 to 2.749 Å).[21] There are two types of Nb–As bonds within the cluster. Nb(1)–As(1–3) bear an average bond distance of 2.571 Å, which is obviously shorter than that in Nb(1)–As(4–6) (2.783 Å in average). As a comparison, the Nb–As bonds in $[NbAs_8]^{3-}$ fall in the range of 2.614–2.637 Å.[15d] Based on the above analysis, the six-coordinated Nb(1) has strong interactions with As(1–3), but relatively weak interactions with As(4–6). The average As–As bond distance in the As_3 triangle is 2.425 Å, comparable to those in $[NbAs_8]^{3-}$ and $[TlAs_7]^{2-}$.[15d,21]

In order to understand the structure and stability of this cluster, quantum chemical calculations were performed on $[As_3Nb(As_3Sn_3)]^{3-}$ and its crystal using density-functional theory (DFT) calculations at the PBE level. As shown in Table S3,† the optimized geometric parameters of $[As_3Nb(As_3Sn_3)]^{3-}$ with C_{3v} symmetry lie in the range of the experimental ones. The calculated HOMO–LUMO energy gap is 1.61 eV, indicating remarkable electronic stability of the cluster. The electronic structure of $[As_3Nb(As_3Sn_3)]^{3-}$ can be interpreted *via* a fragment molecular orbital (MO) approach. As shown in Fig. S8 and S9,† the bonding interactions based on As 4s and Sn 5s atomic orbitals (AOs) play negligible roles in the As_3^{3-} and Sn_3^{2-} fragments, because the bonding and antibonding interactions cancel each other out. Thus, As, Sn, and Nb have three, two, and five valence electrons, respectively, resulting in a system of 32 valence electrons for $[As_3Nb(As_3Sn_3)]^{3-}$, which occupy 16 MOs as shown in Fig. S12.† Note that the As_3^+ and Sn_3^{2-} ions have large HOMO–LUMO gaps (Fig. S8 and S9†) and should be electronically rather stable, in which all the bonding MOs from the radial, tangential, and vertical p-AOs of the three atoms are fully occupied, whereas their corresponding antibonding MOs are empty.

Fig. 2 shows the scalar relativistic (SR) energy levels of $[As_3Nb(As_3Sn_3)]^{3-}$ and its Nb, As_3, and As_3Sn_3 fragments due to orbital interactions. As shown in Fig. S11,† the spin–orbit coupling effects cause little splitting of the SR levels, which will not be discussed. The Nb 5s and 4d AOs transform as a_1 (s) and a_1 (d_{z^2}) + e (d_{xz}, d_{yz}) + e (d_{xy}, $d_{x^2-y^2}$) in C_{3v} symmetry. Based on the MO theory, Nb 5s and 4d AOs will be considerably destabilized through orbital interactions with the As_3 and As_3Sn_3 fragments. As a result, all the five electrons of Nb are lost, leading to an anticipated d^0-complex with a Nb(v) oxidation state. For the top As_3 fragment, the $2a''_2$ and $3e''$ orbitals consisting of As vertical pπ-AOs (Fig. S8†) will overlap directly with the Nb d_{z^2} and (d_{xz}, d_{yz}) AOs, as shown in the con-

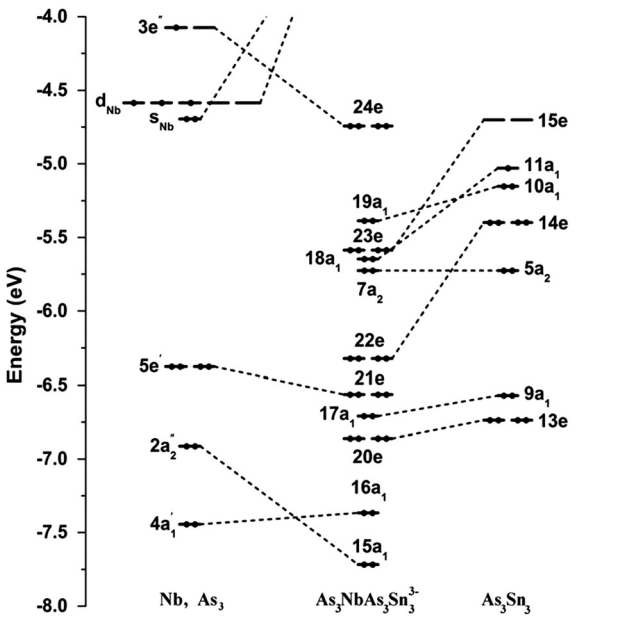

Fig. 2 Energy levels of the scalar-relativistic Kohn–Sham MOs of $[As_3Nb(As_3Sn_3)]^{3-}$ and their correlation with the orbitals of the Nb, As_3, and As_3Sn_3 fragments.

tours of the canonical MOs in Fig. S12,† and get significantly stabilized to become $15a_1$ and 24e (HOMO) in $[As_3Nb(As_3Sn_3)]^{3-}$ (Fig. 2). Because of this stabilization of the 3e″ fragment MOs, the As_3 ring prefers to accept three electrons to fill the HOMO, formally forming an As_3^{3-} trianion in $[As_3Nb(As_3Sn_3)]^{3-}$. On the other hand, the respective orbital interactions between Nb 5s/d_{z^2}, (d_{xy}, $d_{x^2-y^2}$), and (d_{xz}, d_{yz}) orbitals and the $11a_1$, 14e, and 15e fragment orbitals of As_3Sn_3 lead to significant bonding stabilization (Fig. 2), forming the bonding MOs $18a_1$, 22e, and 23e in $[As_3Nb(As_3Sn_3)]^{3-}$ (Fig. S12†). The remarkable bonding stabilization due to orbital interactions of $11a_1$ and 15e of As_3Sn_3 with Nb makes it necessary for As_3Sn_3 to obtain five more electrons to accomplish a stable closed-shell fragment. Consequently, As_3Sn_3 in $[As_3Nb(As_3Sn_3)]^{3-}$ can be viewed formally as a pentavalent ligand with As_3^{3-} and Sn_3^{2-} units. This electron counting scheme accounts for the intrinsic reason why $[As_3Nb(As_3Sn_3)]^{3-}$ exists as a trianion in the synthesized crystal.

The MO analysis of $[As_3Nb(As_3Sn_3)]^{3-}$ (Fig. S12†) supports the above bonding picture, according to which the top As_3^{3-} ligand should formally possess three As=As double bonds, defined by HOMO−10($15a_1$)/HOMO(24e) and HOMO−9($16a_1$)/HOMO−6(21e) (Fig. S12†). The bonding of the Sn_3^{2-} unit in the $As_3Sn_3^{5-}$ ligand should be greater than three Sn–Sn single bonds. These turn out not to be exact, suggesting that the ionic bonding picture is only a zeroth order approximation. The actual bonding in the system is much more covalent, as the calculated atomic charges show (Table S4†). Indeed, on the basis of the latest recommended covalent radii,[22] the top limit of a single bond is 2.42 Å for As–As and 2.80 Å for Sn–Sn, indicating that the effective As–As bond order in the top As_3 ligand in $[As_3Nb(As_3Sn_3)]^{3-}$ (2.416–2.437 Å) is close to a single bond and the Sn–Sn bond order in the As_3Sn_3 ligand is markedly weaker than a single bond (3.123–3.145 Å).

To reconcile the substantial discrepancies between the "formal" and "effective" bond orders in the As_3 and Sn_3 rings in $[As_3Nb(As_3Sn_3)]^{3-}$, it is instructive to take a closer look at all the MOs (Fig. S12†). The majorities of the MOs are highly mixed and involve a secondary component, the latter being responsible for the complicated, inter-layered electronic interactions, which manage to donate/back-donate the electrons between the Nb center and the As_3 and As_3Sn_3 ligands, as well as between the Sn_3 and As_3 units within the As_3Sn_3 ligand. As a consequence, significant amounts of electrons are redistributed from the ligand layers to the interlayer As–Nb, Nb–As′, and As′–Sn links (here As′ labels an As atom in the bottom As_3Sn_3 ligand), whose distances are 2.770–2.791, 2.558–2.584, and 2.735–2.775 Å, respectively. These distances are compared to the upper limit of single bonds, 2.64 Å for As–Nb and 2.75 Å for As–Sn,[15d,21] suggesting remarkable As–Nb/Nb–As′ bonding (probably equivalent to six As–Nb single bonds) and somewhat weaker As′–Sn interaction. The calculated Wiberg bond orders[23] (Table S5†) are fully consistent with the above analysis. In particular, the Wiberg bond order for Nb–As′ is 1.00, despite the fact that not a single Nb–As′ bond can be identified from the MOs (Fig. S12†). In this picture, it is not surprising that Nb–As and Nb–As′ show quite different bond distances. The As and As′ atoms differ in coordination environments and thus show different donor–acceptor properties. The top As_3 ligand appears to be robust, resulting in weaker As–Nb bonds with respect to As′–Nb, as anticipated.

Adaptive natural density partitioning (AdNDP) analysis[24] offers a useful tool to capture the "effective" interlayer As–Nb, Nb–As′, and As′–Sn bonding in $[As_3Nb(As_3Sn_3)]^{3-}$, as well as the reduced As–As, As′–As′, and Sn–Sn bond orders. Fig. 3 illustrates the AdNDP results, which is an alternative, localized view of the true chemical bonding in $[As_3Nb(As_3Sn_3)]^{3-}$ (Fig. S12†). This bonding pattern is relatively simple and straightforward: the Nb center forms six two-center two-electron (2c–2e) As–Nb/As′–Nb σ bonds, whereas the bowl-type As_3Sn_3 ligand is held together by six As′–Nb σ bonds with discernible contributions from Sn (that is, six As′–Nb–Sn 3c–2e σ bonds).[25] As a consequence of electron redistributions, the top As_3 ligand has three 2c–2e σ bonds with a significantly reduced As–As bond order from 2 (Fig. S12†) to 1. For the As_3Sn_3 ligand, the Sn_3 unit is now bound together *via* a single 3c–2e Sn–Sn–Sn σ bond and there appears to be no As′–As′ bonds, because the As′ (valence 3) is associated with one As′–Nb and two As′–Sn σ bonds, whereas the Sn atom (valence 2) forms two Sn–As′ σ bonds. This analysis also indicates the structural integrity of As_3Sn_3 as one ligand, which cannot be further divided into an As_3 ring and a Sn_3 ring, because such an As_3 ring does not exist in the bowl-like As_3Sn_3.

Overall, the only essentially delocalized bond in the system is the 3c–2e Sn–Sn–Sn σ bond (Fig. 3), which is readily traced back to HOMO−1 ($19a_1$) in the canonical MOs (Fig. S12†). As mentioned above, the Sn_3 unit has exhausted all valence electrons for the Sn–As′ σ bonds. Thus the 3c–2e Sn–Sn–Sn σ bond requires two extra electrons, resulting in the Sn_3^{2-} charge state. From this delocalized Sn–Sn–Sn σ bond, one can view

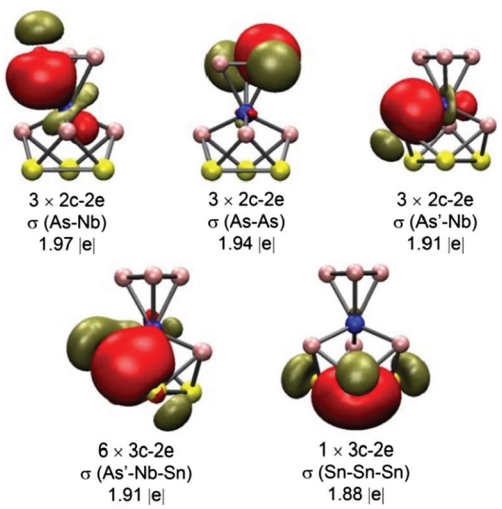

Fig. 3 The AdNDP bonding pattern of $[As_3Nb(As_3Sn_3)]^{3-}$ (isovalue = 0.05 a.u.). Only one bond is shown for each type for clarity. The lone-pair electrons (As 4s and Sn 5s) are not shown. The occupation numbers (ONs) are indicated in the last row.

the Sn_3^{2-} ring as being σ-aromatic,[26] similar to the scenario of cyclopropanyl cations. Such an electron-deficient system is also reminiscent of the salt-like $BaSn_3$ and the organic ligand stabilized $[\{Sn(\mu\text{-}PCy)\}_3]^{2-}$, as well as $[Pb_5\{Mo(CO)_3\}_2]^{4-}$.[27] Compared with benzene and cyclopropanyl cations, a large negative nucleus independent chemical shift (NICS)[28] is obtained at the center of the Sn_3^{2-} ring. The calculated NICS (0) value is −39.55 ppm for the Sn_3^{2-} ring in **1**, whereas they amount to −7.46 and −43.48 ppm for benzene (π aromatic) and cyclopropane (σ aromatic), respectively. The σ-aromaticity in Sn_3^{2-} renders the $As_3Sn_3^{5-}$ ligand σ-aromaticity. While As_3^+ is also aromatic (Fig. S8†) as the cyclic bonding orbitals are all occupied and antibonding orbitals are all vacant, As_3^{3-} with four more electrons added to the degenerate 3e″ antibonding orbitals will cancel the aromaticity. The As_3^{3-} ligand is non-aromatic. In short, $[As_3Nb(As_3Sn_3)]^{3-}$ is a flower-vase shaped cluster, in which a Nb(v) center is sandwiched by a nonaromatic As_3^{3-} ring and a bowl-like, σ-aromatic $As_3Sn_3^{5-}$ ligand.[29] We believe that the non-planarity of the bowl-like $As_3Sn_3^{5-}$ ligand is due to the remarkably strong Nb–As′ σ interactions, which demand suitable As′–As′ distances.

3. Conclusions

Herein we report a novel vase shaped Zintl cluster, $[As_3Nb(As_3Sn_3)]^{3-}$, which has been synthesized and characterized. Quantum chemistry calculations confirm the high stability of the trianion cluster and provide understanding of the bonding essence. There exists a multi-center bonding among Nb–As–Sn and σ-aromaticity for the Sn_3 ring, rendering high stability of the pentavalent As_3Sn_3 bowl as a ligand. Moreover, the present results show that the η^3-As_3 ring is a good trivalent ligand upon coordination with metal d-orbitals. A further study of the reactivity of this new precursor $K_8NbSnAs_5$ and other transition metal organometallics will be interesting.

4. Experimental section

Materials, syntheses, and characterization

All manipulations and reactions were performed under a nitrogen atmosphere using standard Schlenk or glovebox techniques. Ethylenediamine (en) (Aldrich, 99%) and acetonitrile (CH_3CN) (Aldrich, 99%) were freshly distilled by CaH_2 prior to use. Toluene (tol) (Aldrich, 99.8%) was distilled from sodium/benzophenone under dinitrogen and stored under dinitrogen. K (Aldrich, 99%), Na (Aldrich, 99.7%), Nb powder (Aldrich, −200 mesh, 99.5%), Sn (Aldrich, 99.5%), As (Aldrich, 99.999%), CaH_2 (Adamas-beta®, 95%), and benzophenone (Aldrich, 99.5%) were used as received. [2.2.2]crypts[30] (TCI, 98%) were dried in a vacuum for 1 d.

Synthesis of $K_8NbSnAs_5$

Following the synthesis strategy of $K_8NbPbAs_5$ by Sevov *et al.*,[31] we obtained $K_8NbSnAs_5$ by replacing Pb with Sn. The corresponding elements K, Nb, Sn and As were mixed in a molar ratio of 8 : 1 : 1 : 5 and loaded in a tubular tantalum container, which was subsequently arc-welded under an argon atmosphere and sealed in an evacuated quartz tube. The mixture was heated at 750 °C for 72 hours and then cooled to room temperature at a cooling rate of 10 °C h^{-1}. Black crystals were obtained. The powder X-ray diffraction pattern showed a small unknown phase in $K_8NbSnAs_5$ as a precursor; see the ESI (ESI; Fig. S6†).

Synthesis of $[K([2.2.2]crypt)]_3[As_3Nb(As_3Sn_3)]\cdot en\cdot tol$

In a 10 mL vial, 150 mg (0.11 mmol) of $K_8NbSnAs_5$ and 300 mg (0.53 mmol) of [2.2.2]crypt were dissolved in 2 mL of ethylenediamine solution, and the mixture was allowed to stir vigorously for 4 h at room temperature. The resulting dark red solution was subsequently filtered through glass wool and transferred to a test tube, and then carefully layered by toluene (2.5 mL). After 5 days, black rod crystals of $[K([2.2.2]crypt)]_3[As_3Nb(As_3Sn_3)]\cdot en\cdot tol$ appeared on the interfaces of the tube wall (35% based on $K_8NbSnAs_5$). It is worth noting here that a similar strategy was applied in the synthesis of $1\infty[Rb\{NbAs_8\}]^{2-}$, $[Co_2@Sn_{17}]^{5-}$, $[Ni@Sn_9]^{4-}$ and the aforementioned M–Ge–As clusters.[15a,17,32]

X-ray measurement and structure solution of two complexes

Single crystal X-ray diffraction data of $K_8NbSnAs_5$ (Table 1) were collected on a Bruker Apex II CCD diffractometer with graphite-monochromated Mo Kα radiation (λ = 0.71073 Å) at 298 K. Data processing was accomplished with the SAINT program.[33] The structure was solved by direct methods and refined on F^2 by full-matrix least squares using SHELXTL-97.[34] Further details on the crystal structure investigations may be obtained from the Fachinformationszentrum Karlsruhe, 76344 Eggenstein-Leopoldshafen, Germany (Fax: (+49) 7247-808-666; E-mail: crysdata@fiz-karlsruhe.de), on quoting the depository number CSD 428027. Single crystal X-ray diffraction data of $[K([2.2.2]crypt)]_3[As_3Nb(As_3Sn_3)]\cdot en\cdot tol$ (Table 1) were collected

Table 1 X-ray measurement and structure solutions of two complexes

Compound	$C_{59.50}H_{119.50}N_8O_{18}K_3NbSn_3As_6$	As_5K_8NbSn
Formula weight	2250.93	899.00
Crystal system	Monoclinic	Monoclinic
Space group	$P2_1/c$	$C2/c$
a/Å	14.328(3)	31.330(9)
b/Å	23.025(5)	9.395(3)
c/Å	27.224(5)	13.367(4)
α/°	90	90
β/°	97.25(3)	95.423(7)
γ/°	90	90
V	8909(3)	3916.8(18)
Z	4	8
ρ_{calc}/g cm^{-3}	1.678	3.049
$\mu(Mo_{K\alpha})$/mm^{-1}	3.369	11.916
Final R indices ($I > 2\sigma(I)$)	R_1 = 0.0588, wR_2 = 0.1190	R_1 = 0.0382, wR_2 = 0.0620
R indices (all data)	R_1 = 0.1019, wR_2 = 0.1336	R_1 = 0.0696, wR_2 = 0.0711

on a Rigaku RAXIS-RAPID equipped with a narrow-focus, 5.4 kW sealed tube X-ray source (graphite-monochromated Mo Kα radiation, λ = 0.71073 Å) at 123 K. Data processing was accomplished with the PROCESS-AUTO processing program. All non-hydrogen atoms were refined with anisotropic displacement parameters during the final cycles. All hydrogen atoms of the organic molecule were placed by geometrical considerations and were added to the structure factor calculations. CCDC 1012141 contains the supplementary crystallographic data for this paper.

Acknowledgements

This work was supported by the NSF of China (21171162, 21221062, 21573138), Jilin Province Youth Foundation (20130522132JH), SRF for ROCS (Chinese Ministry of Education), and the State Key Laboratory of Quantum Optics and Quantum Optics Devices (KF201402). H. J. Z. gratefully acknowledges the start-up fund from Shanxi University for support. The calculations were performed at the Tsinghua National Laboratory for Information Science and Technology. We thank Prof. Yong Pei for valuable discussions.

Notes and references

1 E. Zintl and A. Harder, *Z. Phys. Chem., Abt. A*, 1931, **154**, 47.
2 (*a*) C. H. E. Belin, J. D. Corbett and A. Cisar, *J. Am. Chem. Soc.*, 1977, **99**, 7163; (*b*) J. D. Corbett and P. A. Edwards, *J. Am. Chem. Soc.*, 1977, **99**, 3313; (*c*) S. C. Critchlow and J. D. Corbett, *Inorg. Chem.*, 1982, **21**, 3286.
3 B. W. Eichhorn and R. C. Haushalter, *J. Am. Chem. Soc.*, 1988, **110**, 8704.
4 (*a*) B. Eichhorn and S. Kocak, *Struct. Bonding*, 2011, **140**, 59; (*b*) S. Scharfe, F. Kraus, S. Stegmaier, A. Schier and T. F. Fässler, *Angew. Chem., Int. Ed.*, 2011, **50**, 3630; (*c*) R. S. P. Turbervill and J. M. Goicoechea, *Chem. Rev.*, 2014, **114**, 10807; (*d*) S. C. Sevov and J. M. Goicoechea, *Organometallics*, 2006, **25**, 5678; (*e*) S. Joseph, M. Hamberger, F. Mutzbauer, O. Härtl, M. Meier and N. Korber, *Angew. Chem., Int. Ed.*, 2009, **48**, 8770; (*f*) F. Fendt, C. Koch, S. Gärtner and N. Korber, *Dalton Trans.*, 2013, **42**, 15548; (*g*) C. Schenk and A. Schnepf, *Angew. Chem., Int. Ed.*, 2007, **46**, 5314; (*h*) C. Schenk, F. Henke, G. Santiso-Quiñones, I. Krossingb and A. Schnepf, *Dalton Trans.*, 2008, 4436; (*i*) N. K. Chaki, S. Mandal, A. C. Reber, M. Qian, H. M. Saavedra, P. S. Weiss, S. N. Khanna and A. Sen, *ACS Nano*, 2010, **4**, 5813; (*j*) S. Mandal, A. C. Reber, M. Qian, R. Liu, H. M. Saavedra, S. Sen, P. S. Weiss, S. N. Khanna and A. Sen, *Dalton Trans.*, 2012, **41**, 12365; (*k*) S. Mandal, A. C. Reber, M.-C. Qian, R. Liu, H. M. Saavedra, S. Sen, P. S. Weiss, S. N. Khanna and A. Sen, *Dalton Trans.*, 2012, **41**, 5454; (*l*) Y. Wang, Q. Qin, J. Wang, R. Sang and L. Xu, *Chem. Commun.*, 2014, **50**, 4181.
5 M. J. Moses, J. C. Fettinger and B. W. Eichhorn, *Science*, 2003, **300**, 778.
6 E. N. Esenturk, J. Fettinger, Y. F. Lam and B. Eichhorn, *Angew. Chem., Int. Ed.*, 2004, **43**, 2132.
7 E. N. Esenturk, J. Fettinger and B. Eichhorn, *J. Am. Chem. Soc.*, 2006, **128**, 9178.
8 J.-Q. Wang, S. Stegmaier, B. Wahl and T. F. Fässler, *Chem. – Eur. J.*, 2010, **16**, 1793.
9 L. F. Cui, X. Huang, L. M. Wang, D. Y. Zubarev, A. I. Boldyrev, J. Li and L. S. Wang, *J. Am. Chem. Soc.*, 2006, **128**, 8390.
10 (*a*) C. M. Knapp, B. H. Westcott, M. A. C. Raybould, J. E. McGrady and J. M. Goicoechea, *Angew. Chem., Int. Ed.*, 2012, **51**, 9097; (*b*) C. M. Knapp, B. H. Westcott, M. A. C. Raybould, J. E. McGrady and J. M. Goicoechea, *Chem. Commun.*, 2012, **48**, 12183.
11 (*a*) L. Xu, A. Ugrinov and S. C. Sevov, *J. Am. Chem. Soc.*, 2001, **123**, 4091; (*b*) N. Korber and F. Richter, *Angew. Chem., Int. Ed. Engl.*, 1997, **36**, 1512; (*c*) J. M. Goicoechea, M. W. Hull and S. C. Sevov, *J. Am. Chem. Soc.*, 2007, **129**, 7885; (*d*) L. G. Perla, A. G. Oliver and S. C. Sevov, *Inorg. Chem.*, 2015, **54**, 872; (*e*) B. Weinert, A. R. Eulenstein, R. Ababei and S. Dehnen, *Angew. Chem., Int. Ed.*, 2014, **53**, 4704.
12 A. Spiekermann, S. D. Hoffmann and T. F. Fässler, *Angew. Chem., Int. Ed.*, 2006, **45**, 3459.
13 (*a*) F. Lips, R. Clérac and S. Dehnen, *Angew. Chem., Int. Ed.*, 2011, **50**, 960; (*b*) F. Lips, M. Hołyńska, R. Clérac, U. Linne, I. Schellenberg, R. Pottgen, F. Weigend and S. Dehnen, *J. Am. Chem. Soc.*, 2012, **134**, 1181; (*c*) B. Weinert, F. Weigend and S. Dehnen, *Chem. – Eur. J.*, 2012, **18**, 13589; (*d*) B. Weinert, F. Müller, K. Harms, R. Clérac and S. Dehnen, *Angew. Chem., Int. Ed.*, 2014, **53**, 11979; (*e*) R. Ababei, W. Massa, B. Weinert, P. Pollak, X. Xie, R. Clérac, F. Weigend and S. Dehnen, *Chem. – Eur. J.*, 2015, **21**, 386.
14 T. F. Fässler and S. D. Hoffmann, *Angew. Chem., Int. Ed.*, 2004, **43**, 6242.
15 (*a*) H. G. v. Schnering, J. Wolf, D. Weber, R. Ramirez and T. Meyer, *Angew. Chem., Int. Ed. Engl.*, 1986, **25**, 353; (*b*) B. W. Eichhorn, S. P. Matamanna, D. R. Gardner and J. C. Fettinger, *J. Am. Chem. Soc.*, 1998, **120**, 9708; (*c*) B. Kesanli, J. Fettinger and B. W. Eichhorn, *J. Am. Chem. Soc.*, 2003, **125**, 7367; (*d*) B. Kesanli, J. Fettinger, B. Scott and B. W. Eichhorn, *Inorg. Chem.*, 2004, **43**, 3840; (*e*) B. Kesanli, J. Fettinger and B. W. Eichhorn, *Angew. Chem., Int. Ed.*, 2001, **40**, 2300.
16 C. B. Benda, M. Waibel and T. F. Fässler, *Angew. Chem., Int. Ed.*, 2015, **54**, 522.
17 S. Mitzinger, L. Broeckaert, W. Massa, F. Weigend and S. Dehnen, *Chem. Commun.*, 2015, **51**, 3866.
18 (*a*) B. M. Cossairt, M.-C. Diawara and C. C. Cummins, *Science*, 2009, **323**, 602; (*b*) B. M. Cossairt, N. A. Piro and C. C. Cummins, *Chem. Rev.*, 2010, **110**, 4164.
19 (*a*) A. Velian and C. C. Cummins, *Chem. Sci.*, 2012, **3**, 1003; (*b*) R. Ahlrichs, D. Fenske, K. Fromm, H. Krautscheid,

U. Krautscheid and O. Treutler, *Chem. – Eur. J.*, 1996, **2**, 238; (*c*) R. Ababei, W. Massa, K. Harms, X. Xie, F. Weigend and S. Dehnen, *Angew. Chem., Int. Ed.*, 2013, **52**, 13544; (*d*) F.-X. Pan, L.-J. Li, Y.-J. Wang, J.-C. Guo, H.-J. Zhai, L. Xu and Z.-M. Sun, *J. Am. Chem. Soc.*, 2015, **137**, 10954.

20 (*a*) Z.-M. Sun, H. Xiao, J. Li and L.-S. Wang, *J. Am. Chem. Soc.*, 2007, **129**, 9560; (*b*) F. S. Kocak, P. Zavalij, Y.-F. Lam and B. W. Eichhorn, *Inorg. Chem.*, 2008, **47**, 3515.

21 C. M. Knapp, J. S. Large, N. H. Rees and J. M. Goicoechea, *Dalton Trans.*, 2011, **40**, 735.

22 (*a*) P. Pyykkö and M. Atsumi, *Chem. – Eur. J.*, 2009, **15**, 12770; (*b*) P. Pyykkö, *J. Phys. Chem. A*, 2015, **119**, 2326.

23 K. B. Wiberg, *Tetrahedron*, 1968, **24**, 1083.

24 (*a*) D. Y. Zubarev and A. I. Boldyrev, *Phys. Chem. Chem. Phys.*, 2008, **10**, 5207; (*b*) D. Y. Zubarev and A. I. Boldyrev, *J. Org. Chem.*, 2008, **73**, 9251; (*c*) W. Huang, A. P. Sergeeva, H. J. Zhai, B. B. Averkiev, L. S. Wang and A. I. Boldyrev, *Nat. Chem.*, 2010, **2**, 202; (*d*) J. M. Mercero, A. I. Boldyrev, G. Merino and J. M. Ugalde, *Chem. Soc. Rev.*, 2015, **44**, 6519.

25 The delocalized 3c–2e As′–Nb–Sn bonds are due to simultaneous participation of Nb $5s/d_{z^2}$, (d_{xz}, d_{yz}), (d_{xy}, $d_{x^2-y^2}$) orbitals in the σ-, out-of-plane π-, and in-plane π-type bonding with the As_3Sn_3 fragment. These 3c–2e bonds correspond to six As′–Sn single bonds expected in the classic Lewis model.

26 (*a*) A. E. Kuznetsov, A. I. Boldyrev, X. Li and L. S. Wang, *J. Am. Chem. Soc.*, 2001, **123**, 8825; (*b*) X. Li, A. E. Kuznetsov, H. F. Zhang, A. I. Boldyrev and L. S. Wang, *Science*, 2001, **291**, 859; (*c*) A. E. Kuznetsov, A. I. Boldyrev, H. J. Zhai, X. Li and L. S. Wang, *J. Am. Chem. Soc.*, 2002, **124**, 11791; (*d*) A. E. Kuznetsov, K. A. Birch, A. I. Boldyrev, X. Li, H. J. Zhai and L. S. Wang, *Science*, 2003, **300**, 622; (*e*) A. I. Boldyrev and L. S. Wang, *Chem. Rev.*, 2005, **105**, 3716; (*f*) A. N. Alexandrova and A. I. Boldyrev, *J. Phys. Chem. A*, 2003, **107**, 554; (*g*) H. J. Zhai, L. S. Wang, A. N. Alexandrova, A. I. Boldyrev and V. G. Zakrzewski, *J. Phys. Chem. A*, 2003, **107**, 9319.

27 (*a*) T. F. Fässler and C. Kronseder, *Angew. Chem., Int. Ed. Engl.*, 1997, **36**, 2683; (*b*) P. Alvarez-Bercedo, A. D. Bond, R. Haigh, A. D. Hopkins, G. T. Lawson, M. McPartlin, D. Moncrieff, M. E. G. Mosquera, J. M. Rawson, A. D. Woodsa and D. S. Wright, *Chem. Commun.*, 2003, 1288; (*c*) L. Yong, S. D. Hoffmann, T. F. Fässler, S. Riedel and M. Kaupp, *Angew. Chem., Int. Ed. Engl.*, 1997, **44**, 2092.

28 (*a*) P. v. R. Schleyer, C. Maerker, A. Dransfeld, H. Jiao and N. J. R. van Eikema Hommes, *J. Am. Chem. Soc.*, 1996, **118**, 6317; (*b*) P. v. R. Schleyer, *Chem. Rev.*, 2005, **105**, 3433; (*c*) M. Sola, F. Feixas, J. O. C. Jimenez-Halla, E. Matito and J. Poater, *Symmetry*, 2010, **2**, 1156; (*d*) P. Jin, F. Li and Z. Chen, *J. Phys. Chem. A*, 2011, **115**, 2402; (*e*) Y. Li, F. Li and Z. Chen, *J. Am. Chem. Soc.*, 2012, **134**, 11269.

29 (*a*) E. Urnėžius, W. W. Brennessel, C. J. Cramer, J. E. Ellis and P. v. R. Schleyer, *Science*, 2002, **295**, 832; (*b*) T. Murahashi, M. Fujimoto, M. Oka, Y. Hashimoto, T. Uemura, Y. Tatsumi, Y. Nakao, A. Ikeda, S. Sakaki and H. Kurosawa, *Science*, 2006, **313**, 1104; (*c*) T. Murahashi, K. Usui, R. Inoue, S. Ogoshi and H. Kurosawa, *Chem. Sci.*, 2011, **2**, 117; (*d*) T. Hatanaka, Y. Ohki and K. Tatsumi, *Angew. Chem., Int. Ed.*, 2014, **53**, 2727.

30 [2.2.2]crypt: 4,7,13,16,21,24-hexaoxa-1,10-diazabicyclo[8.8.8]-hexacosane.

31 F. Gascoin and S. C. Sevov, *Inorg. Chem.*, 2002, **41**, 2820.

32 (*a*) V. Hlukhyy, H. He, L. A. Jantke and T. F. Fässler, *Chem. – Eur. J.*, 2012, **18**, 12000; (*b*) H. He, W. Klein, L.-A. Jantke and T. F. Fässler, *Z. Anorg. Allg. Chem.*, 2014, **640**, 2864; (*c*) M. M. Gillett-Kunnath, J. I. Paik, S. M. Jensen, J. D. Taylor and S. C. Sevov, *Inorg. Chem.*, 2011, **50**, 11695.

33 *SMART and SAINT (software packages)*, Siemens Analytical X-ray Instruments, Inc., Adison, WI, 1996.

34 *SHELXTL Program, version 5.1*, Siemens Industrial Automation, Inc., Madison, WI, 1997.